Enhanced Oxygen Mass Transfer in Aquaculture Using a Low-Cost Nanobubble Fluid Spray System

Muki Satya Permana *, Sugiharto, Toto Supriyono, Fauzi Yusupandi, Anes Inda Rabbika, Turnad Lenggo Ginta

Posted Date: 3 April 2026

doi: 10.20944/preprints202604.0271.v1

Keywords: nanobubble spray system; oxygen mass transfer; aquaculture aeration; dissolved oxygen enhancement; hydrodynamic mass transfer; decentralized aquaculture

 doi:10.20944/preprints202604.0271.v1

Article

Enhanced Oxygen Mass Transfer in Aquaculture Using a Low-Cost Nanobubble Fluid Spray System

Muki Satya Permana [1,*], Sugiharto [1], Toto Supriyono [1], Fauzi Yusupandi [2], Anes Inda Rabbika [3] and Turnad Lenggo Ginta [4]

[1] Department of Mechanical Engineering, Universitas Pasundan, Bandung, Indonesia
[2] Department of Chemical Engineering, Institut Teknologi Sumatera, Lampung, Indonesia
[3] Department of Mechanical Engineering, Universitas Muhammadyah Tasik, Tasik, Indonesia
[4] Research Center for Manufacturing Technology of Production Machinery, National Research and Innovation Agency (BRIN), Tangerang, Indonesia
* Correspondence: muki.satya@unpas.ac.id; Tel.: +62-82120078823

Featured Application

This study presents a low-cost nanobubble spray system for decentralized aquaculture, enabling efficient oxygen transfer under low-power conditions to improve water quality and fish productivity.

Abstract

Dissolved oxygen (DO) management is a primary challenge in intensive aquaculture, where conventional aeration often suffers from high energy costs and low efficiency in decentralized systems. Oxygen transfer kinetics were investigated under oxygen-depleted conditions (initial DO = 2.4 mg L^{-1}) using the dynamic method. The system's performance was characterized through the volumetric mass transfer coefficient (k_La), Specific Oxygen Transfer Efficiency (SOTE), and dimensionless analysis (Reynolds, Schmidt, and Sherwood numbers). After 1 hour of operation, the DO concentration increased to 6.2 mg L^{-1}, achieving a net oxygen transfer of 9.55 ± 0.46 g. The system yielded a kLa of 1.44 h^{-1} (R^2 = 0.97) and a SOTE of 76.4 ± 7.8 gO_2 kWh^{-1}. Dimensionless analysis (Re ≈ 2 x 10^4, Sc ≈ 500, Sh ≈ 682) confirms that oxygen transfer is governed by hydrodynamic-induced interfacial area generation rather than molecular diffusion. Biological validation demonstrated that fish (catfish) grown under nanobubble-assisted conditions achieved a 43% higher growth rate over 17 days compared to non-assisted groups. These findings demonstrate that hydrodynamically controlled nanobubble spray systems provide an energy-efficient and scalable solution for decentralized aquaculture aeration.

Keywords: nanobubble spray system; oxygen mass transfer; aquaculture aeration; dissolved oxygen enhancement; hydrodynamic mass transfer; decentralized aquaculture

1. Introduction

Dissolved oxygen (DO) availability is a critical factor in intensive aquaculture systems because it directly influences fish metabolism, growth performance, and overall pond productivity. Maintaining adequate oxygen levels remains a major challenge, as conventional aeration technologies often require high energy input while providing limited oxygen transfer efficiency. Insufficient DO conditions can induce physiological stress, reduce growth rates, and lead to production losses in aquaculture operations [1–3]. In modern systems such as recirculating aquaculture systems (RAS), DO dynamics are strongly affected by feeding rates, stocking density, water temperature, and aeration performance, making continuous monitoring and control essential [1,2]. In pond-based systems, DO fluctuations are also influenced by diel cycles and temperature variations, which alter the balance between oxygen production and biological consumption [2,3].

 doi:10.20944/preprints202604.0271.v1

Effective DO management has therefore become a central engineering challenge. Oxygen availability in aquaculture is governed by interactions among hydrodynamic conditions, aeration efficiency, and biological demand [4]. Maintaining sufficient DO levels is essential for sustaining fish survival, growth, and economic productivity, particularly for commercially important species such as tilapia and shrimp [5,6]. Conventional aeration systems—including paddlewheel aerators, diffused air systems, and venturi injectors—have been widely implemented to enhance oxygen transfer and mixing. However, these systems often exhibit a trade-off between oxygen transfer performance and energy consumption. The volumetric mass transfer coefficient (kLa) is commonly used to evaluate aeration performance, representing the kinetics of oxygen transfer in gas–liquid systems. Although high-power aeration can rapidly increase DO levels, the associated operational cost becomes a significant constraint, especially in small-scale and decentralized aquaculture systems [1,7–9].

Recent advances in aeration technology have focused on improving system efficiency through optimized design and control strategies. Automated aeration systems and sensor-based monitoring have been proposed to regulate oxygen supply based on real-time DO conditions [10,11]. Additionally, low-power aeration strategies have been explored to reduce energy consumption while maintaining adequate oxygen levels, although optimal configurations remain dependent on hydrodynamic performance [1,12]. Among emerging technologies, nanobubble (NB) systems have attracted considerable attention due to their potential to enhance gas–liquid mass transfer efficiency. Nanobubbles are ultrafine gas bubbles characterized by extremely small diameters and large interfacial surface areas, which can significantly increase oxygen transfer rates compared to conventional aeration systems. Enhanced performance is attributed to prolonged bubble residence time and increased interfacial area, which facilitate oxygen diffusion into the liquid phase [13–15]. Previous studies have demonstrated that nanobubble technology can improve DO concentration and biological responses in aquaculture systems, although performance is strongly influenced by injection configuration and operating conditions [14–16].

Despite these advantages, most existing studies are limited to laboratory-scale systems using specialized nanobubble generators. Such systems may not fully represent practical aquaculture conditions, where simplicity, cost efficiency, and energy consumption are critical considerations. Field-scale implementation of low-power nanobubble systems remains limited, particularly for decentralized pond aquaculture employing spray-based injection mechanisms [13,17,19]. Therefore, this study investigates oxygen transfer enhancement using a low-cost nanobubble fluid spray system designed for circular tarpaulin ponds. The approach integrates experimental DO measurements, estimation of the volumetric mass transfer coefficient (kLa), evaluation of energy performance through specific oxygen transfer efficiency (SOTE), and hydrodynamic analysis using dimensionless parameters. This work aims to provide a practical and scalable engineering framework for improving oxygen transfer efficiency in small-scale aquaculture systems.

2. Materials and Methods

The fluid spray system was constructed using a series of PVC pipes and tubes equipped with a flow control valve and powered by a 125 W electric water pump. The system was operated for 1 h per experimental cycle under controlled conditions. The experimental pond was a circular tarpaulin tank with a diameter of 2 m and a height of 1 m. Initially, dissolved oxygen concentration was measured in the absence of fish. Subsequently, 700 catfish with an initial average length of 13.4 cm were introduced into the pond.

Dissolved oxygen concentration and fish length were measured at day 0, day 7, and day 17. The oxygen concentration was monitored under three conditions:

- Without nanobubble injection
- With air-based nanobubble injection
- With pure oxygen-assisted nanobubble injection

 doi:10.20944/preprints202604.0271.v1

2.1. Experimental Setup

The experimental aquaculture setup used to evaluate the performance of the nanobubble-based fluid spray system is shown in Figure 1. The experimental system consisted of a recirculating aquaculture pond integrated with a low power of nanobubble spray unit. The pond was circular with a diameter of 2 m and a water depth of 0.8 m, corresponding to a total volume of approximately 2512 L. A commercial centrifugal pump (Shimizu PS-128 BIT, 125 W) was used to drive the recirculation flow. Air entrainment and bubble dispersion were induced through flow-driven mechanisms within the recirculation line, generating a fine bubble plume upon discharge into the pond. The system was designed to promote turbulent mixing and enhance gas–liquid interfacial area, which are critical factors governing oxygen transfer performance.

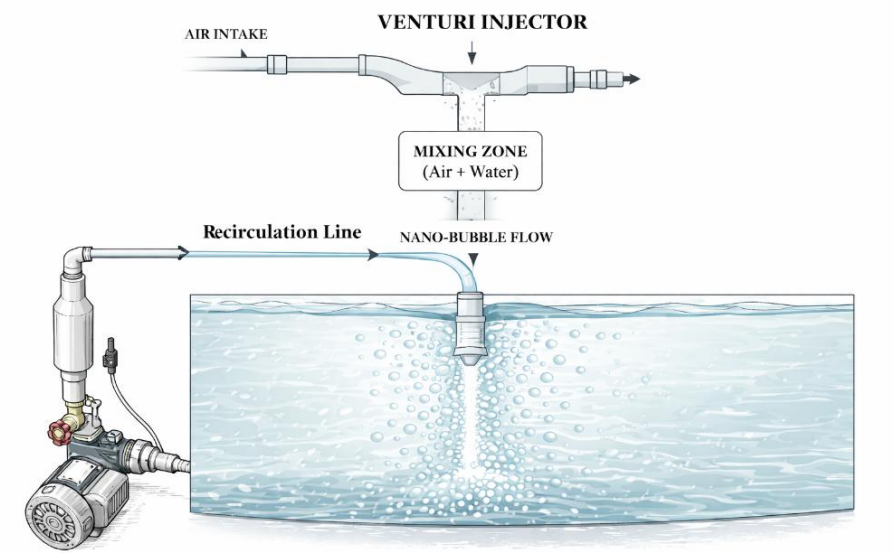

Figure 1. Schematic representation of the nanobubble spray system showing the circulation loop, venturi-induced air entrainment, and bubble dispersion in the aquaculture pond.

2.2. Operating Conditions

The system was operated at a flow rate of approximately 0.16 L s^{-1} for a duration of 3600 s. The initial dissolved oxygen concentration was 2.4 mg L^{-1}, and the saturation concentration was 7.44 mg L^{-1}, under ambient conditions. The saturation dissolved oxygen concentration was determined based on water temperature using standard empirical correlations [20]. All experiments were performed at ambient temperature and atmospheric pressure. No external oxygen source was supplied unless otherwise specified

2.3. Measurement Methods

Dissolved oxygen was measured using a DO-5512SD meter with a resolution of ±0.1 mg L^{-1}. The measurement instruments and specifications are summarized in Table 1.

Table 1. Measurement instruments and specification.

No.	Parameter	Instrument/Specification	Accuracy/Resolution
1.	Pump Power (P)	Shimizu PS-128 BIT (125 W)	±9%
2.	Dissolved Oxygen (DO)	DO-5512SD meter	±0.1 mg L^{-1}
3.	Initial DO (C_0)	2.4 mg L^{-1}	derived from DO meter resolution
4.	Final DO (C_t)	6.2 mg L^{-1}	derived from DO meter resolution
5.	Pond Volume (V)	2512 L (D = 2 m, H = 0.8 m)	±3%
6.	Measurement time (t)	3600 s	±0.1 s
7.	Flowrate (Q)	0.16 (L/s)	used for hydrodynamic analysis

 doi:10.20944/preprints202604.0271.v1

2.4. Oxygen Transfer Analysis

The volumetric mass transfer coefficient (kLa) was determined using the dynamic method based on first-order kinetics. The oxygen transfer process is described by [21,22]:

$$\frac{dC}{dt} = k_L a\,(C^* - C) \quad (1)$$

where C is the dissolved oxygen concentration (mg L^{-1}), C^* is the saturation concentration (7.44 mg L^{-1}), and kLa is the volumetric mass transfer coefficient (h^{-1}). By integrating the equation, the following linear form is obtained:

$$ln\left(\frac{C^* - C_t}{C^* - C_0}\right) = -k_L a t \quad (2)$$

2.5. Specific oxygen transfer efficiency (SOTE)

The oxygen mass transfer and SOTE were calculated based on the measured DO increase and energy consumption. The total oxygen transferred was calculated as:

$$m_{O_2} = (C_{t-} C_0)\, x\, V \quad (3)$$

where V is the pond volume (L).

The SOTE was calculated as:

$$SOTE = \frac{Mass\ of\ oxygen\ transfer}{Electrical\ Energy\ Input} = \frac{m_{O_2}}{P\ x\ t} \quad (4)$$

where P is the pump power (W) and t is the operating time (h). This parameter represents the amount of oxygen transferred per unit energy input.

All experiments were conducted in a single run under controlled conditions, and uncertainty analysis was applied to account for measurement variability.

3. Results

3.1. Overall Oxygen Transfer Behavior and Kinetics

The oxygen transfer performance of the proposed nanobubble spray system was evaluated through the temporal evolution of dissolved oxygen (DO) and its corresponding kinetic behavior. As shown in Figure 2, the DO concentration increased from 2.4 ± 0.1 mg L^{-1} to 6.2 ± 0.1 mg L^{-1} within 3600 s of operation, indicating substantial oxygen transfer under low-power conditions. The calculated volumetric mass transfer coefficient (kLa) was 1.44 h^{-1}, as presented in Figure 3.

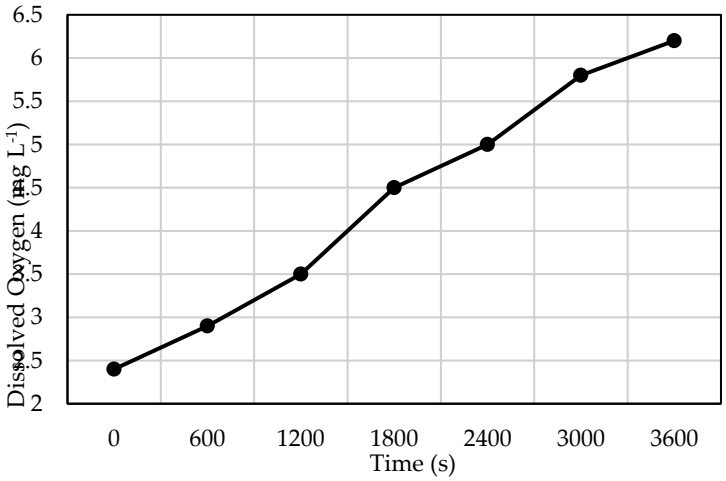

Figure 2. Temporal evolution of dissolved oxygen during nanobubble-assisted aeration, highlighting rapid increase and saturation dynamics.

 doi:10.20944/preprints202604.0271.v1

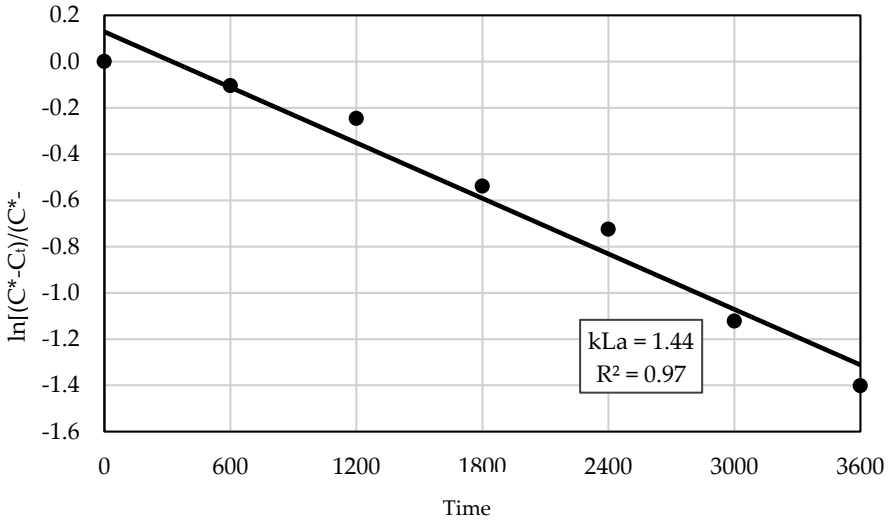

Figure 3. Semi-logarithmic plot for kLa determination showing first-order mass transfer behavior with linear regression ($R^2 = 0.97$).

3.2. Energy Performance (SOTE)

The energy performance of the system was evaluated using the Specific Oxygen Transfer Efficiency (SOTE). This was calculated based on oxygen mass increase and energy input (Eq. 3), yielding:

$$\text{SOTE} = \frac{(6.2 - 2.4)\ \text{mg L}^{-1} \text{ x } 2.512\ \text{m}^3}{125\ W\ x\ 1\ h} = 76.4\ \text{gO2/kWh}$$

3.3. Effect of Gas Composition and Nanobubble Characteristics

The influence of gas composition and nanobubble formation on oxygen transfer was further evaluated. Under non-biological conditions (No Fish), DO increased from 2.4 mg L^{-1} to 6.2 mg L^{-1} using air and further to 11.6 mg L^{-1} with pure oxygen injection. Under biological conditions (Fish), DO increased from 0.5 mg L^{-1} to 0.9 mg L^{-1} (air) and 1.2 mg L^{-1} (pure oxygen). This explanation is presented as shown in Figure 4.

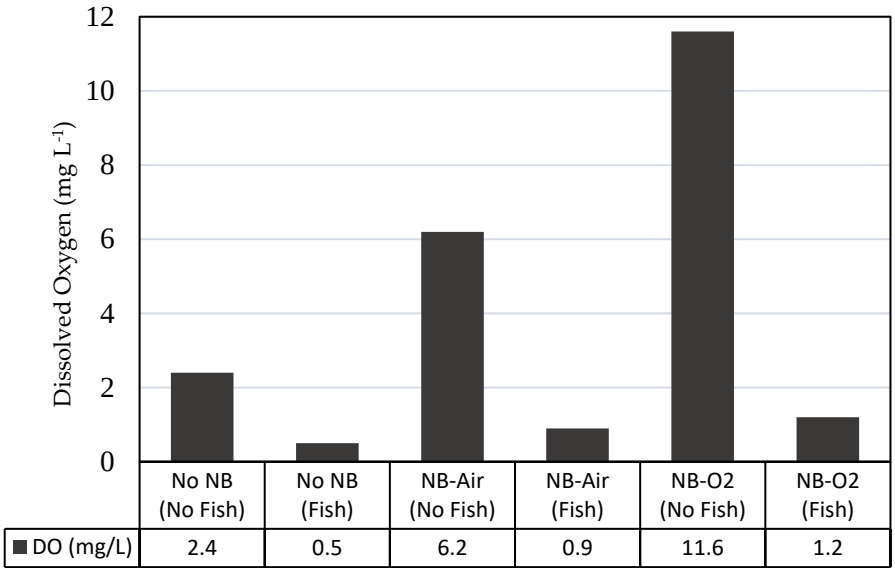

Figure 4. Effect of gas composition and nanobubble (NB) characteristics on dissolved oxygen (DO) concentration under biological (Fish) and non-biological conditions (No Fish).

 doi:10.20944/preprints202604.0271.v1

3.4. Biological Validation of Oxygen Transfer Enhancement

The engineering performance of the system was validated through biological response analysis using catfish growth as an indicator.

Figure 5 presents the variation of average fish length during the 17-day cultivation period with measurements taken at day 0, day 7, and day 17. The results show that fish cultivated under nanobubble-assisted conditions exhibited a 43% higher growth rate over a 17-day period compared to the control group.

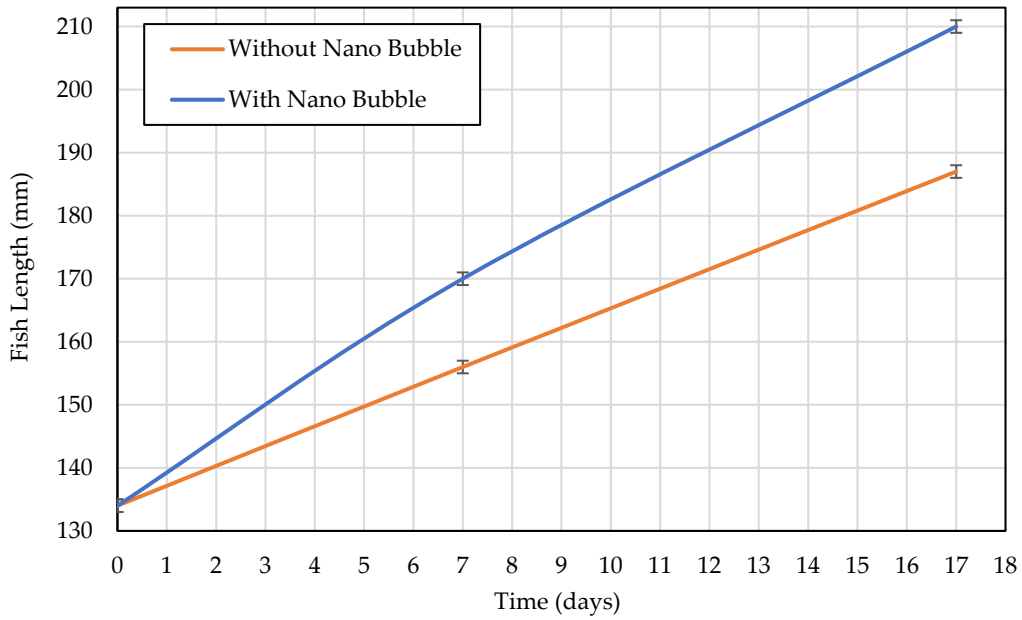

Figure 5. The variation of average fish length during the 17-day cultivation period under two conditions.

3.5. Hydrodynamic and Dimensionless Analysis

The Reynolds number was calculated using $Re = \frac{\rho v d}{\mu}$. With flow rate 0.16 L s^{-1}, d = 0.01 m, ρ = 1000 kg m^{-3}, and μ = 1.0 x 10^{-3} Pa s, the jet velocity was v (Q/A) ≈ 3.18 m s^{-1}, yielding Re ≈ 20,382 which confirms turbulent jet flow. The Schmidt number, calculated as $Re = \frac{\mu}{\rho D}$ with diffusivity of oxygen in water, D = 2.0 x 10^{-9} m^2 s^{-1}, was approximately 500. Using the correlation $Sh = 2 + 0.6Re^{1/2}Sc^{1/3}$, the Sherwood number was estimated as Sh ≈ 682. These values indicate that oxygen transfer in the present system is governed by turbulent mixing and favorable convective mass transfer, while the main limitation remains the available gas–liquid interfacial area rather than intrinsic diffusion kinetics.

3.6. Comparative Performance Evaluation

The obtained kLa (≈1.44 h^{-1}) lies within the range of mechanical aerators (0.3–2.0 h^{-1}) and overlaps with fine-bubble and nanobubble systems (0.5–5.0 h^{-1}). The SOTE (≈ 76.4 gO_2 kWh^{-1}) is significantly lower than industrial systems (500–1500 gO_2 kWh^{-1}).

3.7. Experimental Uncertainty

The uncertainty analysis was performed based on the measurement accuracy and resolution listed in Table 1. The DO uncertainty is based on instrument resolution, while power uncertainties

 doi:10.20944/preprints202604.0271.v1

are derived from manufacturer specifications and flow rate was obtained by volumetric measurement method.

3.7.1. Uncertainty of Oxygen Mass Transfer

The total oxygen mass transferred was determined based on a batch accumulation approach using the change in dissolved oxygen concentration over time.

$$m_{O_2} = \Delta DO \; x \; V$$

where $\Delta DO = C_t - C_0$

The uncertainty in ΔDO was calculated by combining the uncertainties of the initial and final DO measurements:

$$u_{\Delta DO} = \sqrt{(u_{C_0})^2 + (u_{C_t})^2}$$

Given that the DO meter resolution is ±0.1 mg L^{-1}

$$u_{\Delta DO} = \sqrt{(0.1)^2 + (0.1)^2} = 0.1414 \text{ mg } L^{-1}$$

The relative uncertainty is:

$$u_{\Delta DO,rel} = \frac{0.1414}{3.8} = 3.72\%$$

The pond volume uncertainty was assumed to be ±3%, based on geometric measurement limitations. The combined relative uncertainty in oxygen mass transfer is therefore:

$$u_{m,rel} = \sqrt{(3.72\%)^2 + (3\%)^2} = 4.78\%$$

The absolute uncertainty is:

$$u_m = 9.55 \times 4.78\% = 0.46 \text{ g}$$

Thus, the oxygen mass transfer is:

$$m_{O_2} = 9.55 \pm 0.46 \; g$$

3.7.2. Uncertainty of SOTE

The SOTE uncertainty is influenced by the uncertainties in oxygen mass transfer and electrical energy input. The relative uncertainty is expressed as:

$$u_{SOTE,rel} = \sqrt{(u_m)^2 + (u_E)^2}$$

The uncertainty in electrical energy is primarily governed by the pump power measurement, estimated at ±9%. The contribution of time measurement uncertainty is negligible.

$$u_{SOTE,rel} = \sqrt{(4.78)^2 + (9)^2} = 10.19\%$$

The absolute uncertainty is:

$$su_{SOTE} = 76.4 \times 10.19\% = 7.8 \text{ gO2/kWh}$$

Thus, the final SOTE value is:

$$\text{SOTE} = 76.4 \pm 7.8 \text{ gO2/kWh}$$

4. Discussion

4.1. Overall Oxygen Transfer Behavior and Kinetics

From Figure 2, the DO profile exhibits a characteristic non-linear trend with two distinct regimes. In the initial stage, a rapid increase in DO is observed due to a large concentration driving force, whereas in the later stage the rate of increase gradually decreases as the system approaches saturation. This behavior is consistent with classical gas–liquid mass transfer theory, where the oxygen transfer rate is governed by the difference between the saturation concentration (C*) and the instantaneous concentration (C_t) [22,23]. The kinetic analysis confirms this observation. The semi-

 doi:10.20944/preprints202604.0271.v1

logarithmic transformation of the mass transfer equation yielded a strong linear relationship (R^2 = 0.97), indicating that the system follows first-order mass transfer kinetics (Figure 3). The linear regression of the transformed data yielded a slope corresponding to kLa. The calculated volumetric mass transfer coefficient (kLa) was 1.44 h^{-1}, demonstrating effective oxygen transfer performance (Eq. 2).

This value falls within the range reported for conventional aeration systems, suggesting that the proposed system achieves comparable mass transfer capability despite its simplified and low-energy configuration. The high linearity confirms that oxygen transfer in the system follows first-order mass transfer kinetics, consistent with conventional aeration models [24,25]. The slight deviation from ideal linearity can be attributed to minor hydrodynamic fluctuations and measurement uncertainty, which are typical in open aquaculture systems. From a physical perspective, the obtained kLa value indicates that the system achieves effective oxygen transfer performance comparable to conventional mechanical aerators, despite operating at significantly lower power input. This highlights the role of hydrodynamic enhancement, where turbulent jet-induced mixing and bubble fragmentation increase the effective interfacial area.

4.2. Energy Performance Interpretation

Although the obtained SOTE is lower than values reported for industrial aeration systems (typically 500–1500 gO_2 kWh^{-1}), direct comparison must consider differences in system scale and operating conditions [26,27]. Industrial systems are optimized for maximum oxygen transfer using pressurized gas injection and specialized diffusers, whereas the present system is designed for low-power, decentralized applications.

In this context, the measured SOTE should not be interpreted as a limitation, but rather as an indication of system design philosophy. A portion of the input energy is utilized for bulk fluid circulation and mixing, which enhances oxygen distribution but does not directly maximize oxygen transfer efficiency. This distinction highlights the importance of application-oriented performance rather than purely energy-normalized metrics.

4.3. Role of Gas Composition and Nanobubbles

This result clearly indicates that oxygen transfer is strongly influenced by gas partial pressure. According to Henry's law, the equilibrium concentration (C*) is proportional to the gas partial pressure [28]. In addition to thermodynamic effects, nanobubbles contribute significantly to oxygen transfer enhancement. Due to their small size, high stability, and low buoyancy, nanobubbles exhibit prolonged residence time and large specific interfacial area. The combined effect of increased partial pressure and enhanced interfacial area results in a synergistic improvement in oxygen transfer performance. Under biological conditions, DO increased from 0.5 mg L^{-1} to 0.9 mg L^{-1} (air) and 1.2 mg L^{-1} (pure oxygen), indicating that the system remains effective even in the presence of continuous oxygen consumption.

This confirms that the nanobubble spray system is capable of maintaining oxygen availability under realistic aquaculture conditions. Overall, the results indicate that oxygen transfer enhancement is governed by a combination of hydrodynamic effects and thermodynamic driving forces. While turbulent mixing and bubble fragmentation increase interfacial area, gas composition determines the maximum achievable oxygen concentration, highlighting the coupled role of fluid dynamics and gas properties in controlling system performance.

4.4. Biological Implications

This improvement can be directly attributed to the enhanced dissolved oxygen availability in the system. As demonstrated in Section 3.1, increased DO levels and kLa values provide a more favorable environment for fish metabolism. Adequate oxygen availability supports essential physiological processes, including respiration, feed conversion, and energy utilization [1,2]. Under

 doi:10.20944/preprints202604.0271.v1

low DO conditions, fish experience metabolic stress that reduces feeding efficiency and growth performance. Therefore, the observed increase in growth rate confirms that improved oxygen transfer has a direct and measurable impact on aquaculture productivity. These findings demonstrate that the proposed system is not only effective from an engineering perspective but also delivers practical benefits in real aquaculture applications.

4.5. Hydrodynamic Interpretation

The dimensionless parameters, including Reynolds number (Re), Schmidt number (Sc), and Sherwood number (Sh), were calculated based on classical transport phenomena theory [29,30]. The Sherwood number was estimated using an empirical correlation for convective mass transfer in turbulent flow conditions. The correlation $Sh = 2 + 0.6Re^{1/2}Sc^{1/3}$, is widely used for describing gas–liquid mass transfer around dispersed bubbles and turbulent flow systems [29,31].

The estimated Reynolds number (Re ≈ 2 x 10^4) indicates a turbulent flow regime, which promotes strong mixing and enhances bubble fragmentation. This condition is favorable for increasing the gas–liquid interfacial area. The Schmidt number (Sc ≈ 500) reflects the dominance of liquid-phase diffusion resistance typical for oxygen transfer in water. The corresponding Sherwood number (Sh ≈ 682) suggests enhanced interfacial mass transfer promoted by hydrodynamic mixing and bubble fragmentation. Based on these dimensionless parameters, the conceptual mechanism of oxygen transfer enhancement in the nanobubble spray system can be interpreted as illustrated in Figure 6.

These results indicate that the system operates under conditions where hydrodynamic effects play a dominant role in mass transfer enhancement. The turbulent jet generated by the system increases shear forces, leading to bubble breakup and improved dispersion. This process significantly increases interfacial area, which directly influences kLa. Therefore, oxygen transfer performance is primarily controlled by hydrodynamic conditions rather than intrinsic diffusion limitations.

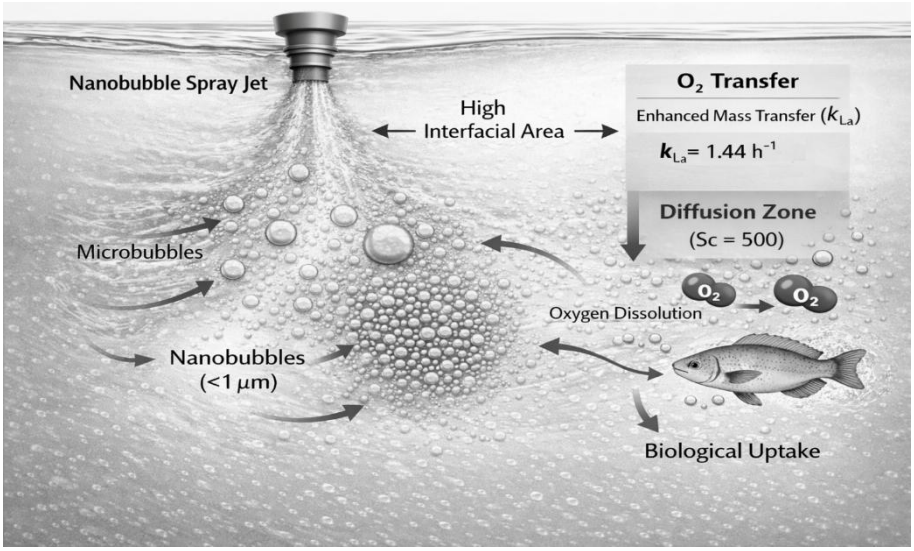

Figure 6. Hydrodynamic mechanism of oxygen transfer enhancement in the nanobubble fluid spray system.

4.6. Comparative Interpretation

The performance of the present system is benchmarked against reported aeration technologies in Table 2. The obtained kLa (≈1.44 h^{-1}) lies within the range of mechanical aerators (0.3–2.0 h^{-1}) and overlaps with fine-bubble and nanobubble systems (0.5–5.0 h^{-1}), indicating comparable hydrodynamic mixing performance [21,26,32]. In contrast, the SOTE (≈ 76.4 gO_2 kWh^{-1}) is significantly lower than industrial systems (500–1500 gO_2 kWh^{-1}), reflecting the low-power, non-pressurized, and decentralized configuration of the system [26,27]. Unlike industrial aerators

 doi:10.20944/preprints202604.0271.v1

designed for maximum efficiency, the present system prioritizes simplicity, low cost, and field applicability.

The results suggest that the system is hydrodynamically effective but interfacially limited, where strong turbulent mixing enhances kLa, while limited gas–liquid interfacial area constrains SOTE.Despite this, the system achieves functional oxygenation (DO increase from 2.4 to 6.2 mg L^{-1}) and improved biological performance, demonstrating its suitability for small-scale aquaculture applications. Overall, the comparison indicates that performance in decentralized systems is governed more by hydrodynamic optimization than by energy input, highlighting interfacial enhancement as the primary pathway for further improvement.

Table 2. Comparative benchmarking of oxygen transfer performance with literature data.

System Type	kLa (h^{-1})	SOTE (gO_2/kWh)	Scale	Reference
Fine bubble diffuser	0.5 – 5.0	800 – 1500	Wastewater plant	[27,36]
Mechanical surface aerator	0.3 – 2.0	500 – 1200	Large pond	[26]
Coarse bubble aerator	0.2 – 1.5	400 – 900	Municipal WWTP	[21]
Venturi injector	0.1 – 0.8	200 – 600	Small systems	[37]
Industrial nanobubble system	0.5 – 3.0	600 – 1300	Treatment plant	[32]
Microbubble generator	0.4 – 2.5	500 – 1100	Lab-scale	[38]
Air pump	0.05 – 0.3	50 – 200	Small-scale air pump	[39]
Nanobubble spray system (this study)	**≈ 1.44**	**≈ 76.4**	2.5 m^3 pond	Present study

4.7. Engineering Interpretation and Uncertainty

The uncertainty analysis was performed based on the measurement accuracy and resolution listed in Table 1. The DO uncertainty is based on instrument resolution, while power uncertainties are derived from manufacturer specifications and flow rate was obtained by volumetric measurement method. The reliability of the experimental results was assessed through uncertainty analysis using the Root Sum Square (RSS) method [33,34]. The calculated uncertainties were 4.78% for oxygen transfer and 10.19% for SOTE, which fall within acceptable ranges for field-scale experiments [33–35].

The dominant source of uncertainty originates from power measurement, while the contribution from DO measurement is relatively small due to the significant concentration difference observed in the system. This confirms that the experimental data are sufficiently reliable for engineering interpretation. From an engineering perspective, the results indicate that system performance is primarily limited by interfacial area rather than diffusion kinetics. This suggests that future optimization should focus on improving bubble generation and dispersion, for example through nozzle design or multi-jet configurations, rather than increasing energy input.

Overall, the integration of hydrodynamic analysis, kinetic modeling, and biological validation demonstrates that efficient oxygen transfer can be achieved through system design optimization, providing a scalable and energy-efficient solution for aquaculture applications. Unlike industrial aerators designed for maximum efficiency, the present system prioritizes simplicity, low cost, and field applicability. The results suggest that the system is hydrodynamically effective but interfacially limited. Despite this, the system achieves functional oxygenation and improved biological performance.

5. Conclusions

This study demonstrates that a low-cost nanobubble fluid spray system can effectively enhance oxygen mass transfer in aquaculture ponds under low-power operating conditions. Operating at 125 W and a flow rate of approximately 0.16 L s^{-1}, the system increased dissolved oxygen concentration from 2.4 mg L^{-1} to 6.2 mg L^{-1} within 3600 s, confirming its capability to improve oxygen availability under oxygen-depleted conditions. The estimated volumetric mass transfer coefficient (kLa ≈ 1.44 h^{-1})

 doi:10.20944/preprints202604.0271.v1

indicates that the system achieves moderate oxygen transfer performance comparable to small-scale aeration technologies. The observed enhancement is primarily attributed to increased gas–liquid interfacial area and improved bubble dispersion generated by shear-induced fragmentation in the spray jet. These results suggest that oxygen transfer performance in low-power systems is governed more by hydrodynamic mechanisms and interfacial engineering than by energy input alone.

From an engineering perspective, the proposed system provides a practical and scalable solution for decentralized aquaculture applications, where energy efficiency and system simplicity are critical. Although the absolute oxygen transfer capacity remains lower than that of industrial aeration systems, the ability to sustain oxygen transfer under constrained power conditions highlights its potential for small-scale pond operations. Future work should focus on optimizing nozzle design, increasing bubble dispersion density, and conducting replicated field-scale validation to further improve system performance and reliability.

Acknowledgments: The authors gratefully acknowledge the financial support provided by the Holistic Village Development and Empowerment *(PHP2D) Ministry of Education, Culture, Research, and Technology, Directorate General of Higher Education, Indonesia.* The authors sincerely thank Mr. Hendar Kadarusman, Program Independent Marine and Fisheries Training Center (P2MPK – Tunas Mina Lestari), and Mr. Eman, Head of Babakan Village, Ciparay District, Bandung Regency, for their valuable support during the research implementation. The authors also extend their appreciation to all individuals who contributed to the successful completion of this study.

References

1. Boyd, C. E., Torrans, E. L., & Tucker, C. S. (2017). Dissolved Oxygen and Aeration in Ictalurid Catfish Aquaculture. *Journal of the World Aquaculture Society*, *49*(1), 7–70. https://doi.org/10.1111/jwas.12469
2. Elnady, M., Elwahed, R. A., & Gad, G. (2016). Effect of Dietary Protein Levels on Dissolved Oxygen Dynamics and Growth Performance of Nile Tilapia. *Egyptian Journal of Agricultural Sciences*, *67*(1), 42–53. https://doi.org/10.21608/ejarc.2016.212896
3. Yanuhar, U., Musa, M., Evanuarini, H., Wuragil, D. K., & Permata, F. S. (2022). Water Quality in Koi Fish (Cyprinus Carpio) Concrete Ponds With Filtration in Nglegok District, Blitar Regency. *Universal Journal of Agricultural Research*, *10*(6), 814–820. https://doi.org/10.13189/ujar.2022.100619
4. Balami, S. (2021). Recirculation Aquaculture Systems: Components, Advantages, and Drawbacks. *Tropical Agroecosystems*, *2*(2), 104–109. https://doi.org/10.26480/taec.02.2021.104.109
5. Abdullah, S. (2019). Environmental Impacts of Commercial Shrimp Farming in Coastal Zone of Bangladesh and Approaches for Sustainable Management. *International Journal of Environmental Sciences & Natural Resources*, *20*(3). https://doi.org/10.19080/ijesnr.2019.20.556038
6. Laktuka, K., Kalnbaļķīte, A., Sniega, L., Logins, K., & Lauka, D. (2023). Towards the Sustainable Intensification of Aquaculture: Exploring Possible Ways Forward. *Sustainability*, *15*(24), 16952. https://doi.org/10.3390/su152416952
7. Dayrit, G. B., Cruz, E. M. V, Rodkhum, C., Mabrok, M., Ponza, P., & Santos, M. D. (2023). Potential Influence of Shading in Freshwater Ponds on the Water Quality Parameters and the Hematological and Biochemical Profiles of Nile Tilapia (Oreochromis Niloticus Linnaeus, 1758). *Fishes*, *8*(6), 322. https://doi.org/10.3390/fishes8060322
8. Han, P., Lu, Q., Fan, L., & Zhou, W. (2019). A Review on the Use of Microalgae for Sustainable Aquaculture. *Applied Sciences*, *9*(11), 2377. https://doi.org/10.3390/app9112377
9. Agus, M., Darmanto, Y. S., & Prayitno, S. B. (2016). The Dynamics of Water Quality Soft-Shelled Crab Aquaculture in Pemalang Regency, Middle Java, Indonesia. *International Journal of Science and Research (Ijsr)*, *5*(2), 1448–1451. https://doi.org/10.21275/v5i2.nov161437
10. Vo, T. T. E., Ko, H., Huh, J., & Park, N. (2021). Overview of Solar Energy for Aquaculture: The Potential and Future Trends. *Energies*, *14*(21), 6923. https://doi.org/10.3390/en14216923
11. Chellapandi, P. (2021). Development of Top-Dressing Automation Technology for Sustainable Shrimp Aquaculture in India. *Discover Sustainability*, *2*(1). https://doi.org/10.1007/s43621-021-00036-9

 doi:10.20944/preprints202604.0271.v1

12. Beg, M. M., Roy, S. M., Kar, A., Mukherjee, C. K., Bhagat, S., & Tanveer, M. (2024). Study on Recirculating Aquaculture System (RAS) in Organic Fish Production. *Iop Conference Series Earth and Environmental Science*, *1391*(1), 12013. https://doi.org/10.1088/1755-1315/1391/1/012013
13. Mauladani, S., Rahmawati, A. I., Absirin, M. F., Saputra, R. N., Pratama, A. F., Hidayatullah, A., Dwiarto, A., Syarif, A. F., Junaedi, H., Cahyadi, D., Saputra, H. K. H., Prabowo, W. T., Kartamiharja, U. K. A., Noviyanto, A., & Rochman, N. T. (2020). Economic Feasibility Study of Litopenaeus Vannamei Shrimp Farming: Nanobubble Investment in Increasing Harvest Productivity. *Jurnal Akuakultur Indonesia*, *19*(1), 30–38. https://doi.org/10.19027/jai.19.1.30-38
14. Tran, N. L. H., Lam, T. Q., Duong, P. V. Q., Doan, L., Vu, M. P., Nguyen, K. H. P., & Nguyen, K. T. (2023). Review on the Significant Interactions Between Ultrafine Gas Bubbles and Biological Systems. *Langmuir*, *40*(1), 984–996. https://doi.org/10.1021/acs.langmuir.3c03223
15. Nghĩa, N. H., Van, P. T., Giang, P. T., Hanh, N. T., St-Hilaire, S., & Domingos, J. A. (2021). Control Of<i>Vibrio</I><i>parahaemolyticus</I>(AHPND Strain) and Improvement of Water Quality Using Nanobubble Technology. *Aquaculture Research*, *52*(6), 2727–2739. https://doi.org/10.1111/are.15124
16. Dien, L. T., Linh, N. V, Sangpo, P., Senapin, S., St-Hilaire, S., Rodkhum, C., & Dong, H. T. (2021). Ozone Nanobubble Treatments Improve Survivability of Nile Tilapia (Oreochromis Niloticus) Challenged With a Pathogenic Multi-drug-resistant Aeromonas Hydrophila. *Journal of Fish Diseases*, *44*(9), 1435–1447. https://doi.org/10.1111/jfd.13451
17. Wang, S., Liu, Y., Lyu, T., Pan, G., & Li, P. (2020). Aquatic Macrophytes in Morphological and Physiological Responses to the Nanobubble Technology Application for Water Restoration. *Acs Es&t Water*, *1*(2), 376–387. https://doi.org/10.1021/acsestwater.0c00145
18. Domingos, J. A., Huang, Q., Liu, H., Dong, H. T., Khongcharoen, N., Van, P. T., Nghĩa, N. H., Giang, P. T., Viet, P. T., & St-Hilaire, S. (2021). *Air-Nanobubbles Ineffective to Reduce Pathogenic Bacteria in Fresh and Brackish Waters*. https://doi.org/10.1101/2021.08.27.457885
19. Chary, K., Brigolin, D., & Callier, M. D. (2022). Farm-scale Models in Fish Aquaculture – An Overview of Methods and Applications. *Reviews in Aquaculture*, *14*(4), 2122–2157. https://doi.org/10.1111/raq.12695
20. Jia, M., Farid, M. U., Kharraz, J. A., Kumar, N. M., Chopra, S. S., Jang, A., Chew, Y. M. J., Khanal, S. K., Chen, G., & An, A. K. (2023). Nanobubbles in Water and Wastewater Treatment Systems: Small Bubbles Making Big Difference. *Water Research*, *245*, 120613. https://doi.org/10.1016/j.watres.2023.120613
21. American Public Health Association (APHA), (2017). Standard Methods for the Examination of Water and Wastewater (23rd ed.). Washington, DC: APHA
22. Metcalf & Eddy Inc. George Tchobanoglous et al. Wastewater Engineering: Treatment and Resource Recovery, McGraw-Hill Education (2014). ISBN: 978-0-07-340118-8
23. Lekang, O. I. (2007). Aquaculture Engineering. Blackwell Publishing.
24. ASCE 18-96: Standard Guidelines for In-Process Oxygen Transfer Testing
25. Chemical Engineering Journal, Zhang et al., (2016) — Microbubble mass transfer enhancement
26. Separation and Purification Technology, Li et al., (2019) — Nanobubble oxygen dissolution
27. Boyd, C.E. and Tucker, C.S. (1998) Pond Aquaculture and Water Quality Management. Kluwer Academic Pub., London, 44-48. https://doi.org/10.1007/978-1-4615-5407-3
28. D Rosso, LE Larson, MK Stenstrom, Aeration of large-scale municipal wastewater treatment plants: state of the art (2008), Water Science and Technology,
29. Frank R. Spellman, The Science of Water, Concepts and Applications, 2nd Ed., (2007), https://doi.org/10.1201/9781420055450
30. Bird, R., Stewart, W. and Lightfoot, E. (2002) Transport Phenomena. 2nd Edition, John Wiley and Sons, New York.
31. Incropera, F. P., DeWitt, D. P., Bergman, T. L., & Lavine, A. S. (2007). Fundamentals of Heat and Mass Transfer (6th ed.). Hoboken, NJ: John Wiley & Sons
32. Coulson, J.M., and Richardson, J.F. (2005). "Chemical Engineering", 4th ed, vol. 6, Pergamon Press, Oxford
33. Hideki Tsuge, (2014), Micro- and Nanobubbles: Fundamentals and Applications, Pan Stanford Publishing
34. Holman, J. P. (2012). Experimental Methods for Engineers (8th ed.). McGraw-Hill Education.

 doi:10.20944/preprints202604.0271.v1

35. Taylor, J. R. (1997). An Introduction to Error Analysis: The Study of Uncertainties in Physical Measurements (2nd ed.). University Science Books.
36. ASME PTC 19.1 (1998). Test Uncertainty, Supplement to ASME Performance Test Codes
37. Boyd, C.E. (2020). Water Quality: An Introduction (2nd ed.). Springer.
38. ASCE 2-06 (2007). Measurement of Oxygen Transfer in Clean Water (ASCE/EWRI 2-06). Reston, VA: American Society of Civil Engineers.
39. Agarwal, A., Ng, W.J. and Liu, Y. (2011) Principle and Applications of Microbubble and Nanobubble Technology for Water Treatment. Chemosphere, 84, 1175-1180. http://dx.doi.org/10.1016/j.chemosphere.2011.05.054
40. Michael B. Timmons; James M. Ebeling (2013), Recirculating Aquaculture, 3rd Edition, Ithaca Publishing Company, LLC.
41. Xu, Y., Li, L., Lou, S., Tian, J., Sun, S.-H., Li, X., & Li, Y. (2022). Effects of Nano-Aerators on Microbial Communities and Functions in the Water, Sediment, and Shrimp Intestine in Litopenaeus Vannamei Aquaculture Ponds. *Microorganisms*, *10*(7), 1302. https://doi.org/10.3390/microorganisms10071302
42. Das, S. K., Mondal, B., Sarkar, U. K., Das, B. K., & Borah, S. (2022). Understanding and Approaches Towards Circular Bio-economy of Wastewater Reuse in Fisheries and Aquaculture in India: An Overview. *Reviews in Aquaculture*, *15*(3), 1100–1114. https://doi.org/10.1111/raq.12758
43. English, N. J. (2022). Sustainable Exploitation and Commercialization of Ultradense Nanobubbles: Reinventing Liquidity. *Acs Sustainable Chemistry & Engineering*, *10*(11), 3383–3386. https://doi.org/10.1021/acssuschemeng.2c01058
44. Mehrim, A. I., & Refaey, M. M. (2023). An Overview of the Implication of Climate Change on Fish Farming in Egypt. *Sustainability*, *15*(2), 1679. https://doi.org/10.3390/su15021679
45. Nisar, U., Peng, D., Mu, Y., & Sun, Y. (2022). A Solution for Sustainable Utilization of Aquaculture Waste: A Comprehensive Review of Biofloc Technology and Aquamimicry. *Frontiers in Nutrition*, *8*. https://doi.org/10.3389/fnut.2021.791738